LC-REP-2013-006

Study of $H \to \mu^+\mu^-$ at $\sqrt{s} = 1$ TeV at the ILC

Constantino Calancha
High Energy Accelerator Research Organization (KEK), Tsukuba, Japan
calancha@post.kek.jp

April 19, 2013

Abstract

The statistical uncertainty of $\sigma(\nu_e\bar{\nu}_e\mathrm{H}) \cdot Br(\mathrm{H} \to \mu^+\mu^-)$ for a 125 GeV/c^2 Standard Model Higgs boson is evaluated, in the context of the 1 TeV ILC [1] e^+e^- linear collider with beam state polarisation (P_{e^-}, P_{e^+})=(-0.8,+0.2), and a total integrated luminosity of 500 fb^{-1}. The study is performed in the ILD [2] detector concept using full simulation. All relevant Standard Model backgrounds are taken into account. The effect of the underlying $\gamma\gamma \to$ hadrons is taken into account by overlaying realistic amounts of $\gamma\gamma \to$ hadrons onto both signal and background events. The cross section times the branching ratio can be measured with a statistical accuracy of 44 ± 3 %.

Contents

1 Introduction

Figure 1: Higgs couplings to SM particles as a function of their masses (left) Higgs branching ratios as a function of the Higgs mass (right).

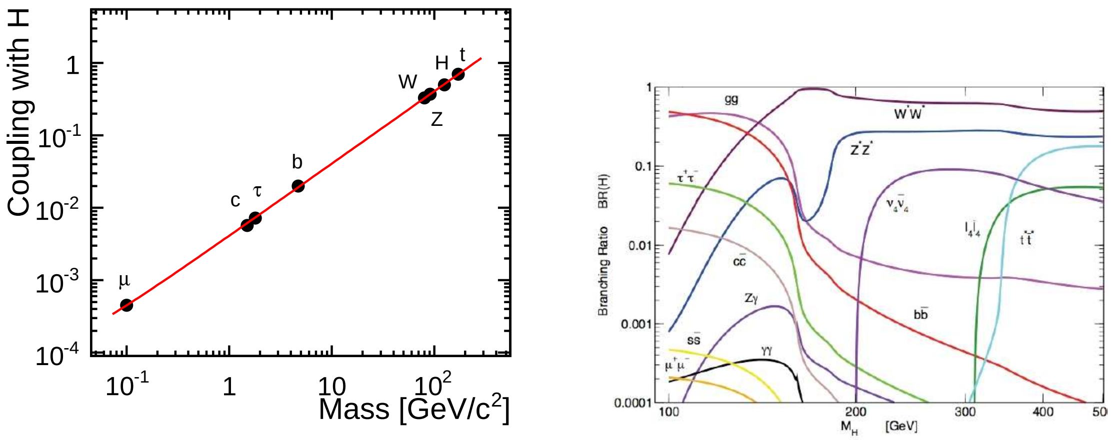

The SM predicts a linear relation between Higgs couplings to SM particles and their masses (Fig. 1). A deviation from this prediction would be a strong indication of new physics. The precise measurement of those couplings is one of the main goals of the ILC physics program.

The recent discovery at ILC of a higgs-like boson with a mass $\sim$ 125 GeV/c^2 makes possible to study many branching ratios of the decay of this boson at the ILC (Fig. 1).

In this note we study $\nu_e\bar{\nu}_e\mathrm{H}, \mathrm{H} \rightarrow \mu^+\mu^-$ at 1 TeV and beam state polarisation (P_{e^-}, P_{e^+})=(-0.8,+0.2), and we determine the expected statistical uncertainty for $\sigma(\nu_e\bar{\nu}_e\mathrm{H}) \cdot Br(\mathrm{H} \rightarrow \mu^+\mu^-)$.

The measurement $\nu_e\bar{\nu}_e\mathrm{H}, \mathrm{H} \rightarrow \mu^+\mu^-$ is quite challenging due to the very low branching ratio Br($\mathrm{H} \rightarrow \mu^+\mu^-$), only 0.02% for a Higgs boson mass of 125 GeV/c^2. After recording 500 fb^{-1} of data with beam polarization state (P_{e^-}, P_{e^+})=(-0.8,+0.2) we expect only 45 $\nu_e\bar{\nu}_e\mathrm{H}, \mathrm{H} \rightarrow \mu^+\mu^-$ events. For the right-handed beam polarisation state (P_{e^-}, P_{e^+})=(+0.8,-0.2) we expect less than 4 events.

2 Software

The event samples used in this analysis were created in the context of the ILD DBD mass production. The event generation is performed using `WHIZARD` [3] v1.95. The fragmentation is taken by `PYTHIA` [4]. The decays of τ leptons are handled by `TAUOLA` [5]. The simulation of the ILD detector is carry out with `GEANT4` [6]. Since the events are generated as head-on collisions in `WHIZARD`, the crossing angle of 7 mrad is taken into account in the simulation step by boosting all particles accordingly. The event reconstruction is perform inside `ILCSOFT` [7] v01-16 framework. The analysis is done using `ROOT` [8] v5.32.00 and the `TMVA` [9] and `RooFit` [10] v3.50 software packages.

3 Event Samples

This section introduces the different samples used in the analysis. Table 1 lists the cross sections and the generated luminosity for all processes. Samples ea_ell, ae_ell, aa_4f and 5f were generated with fast simulation [11]. All the other samples were fully simulated. In Appendix A it is described the actual final state for every considered process.

Processes	σ [fb]	L[ab^{-1}]
Full Simulation		
hmumu (signal)	0.089	64.8
4f_sznu_l	254.9	0.99996
4f_zzorww_l	190.9	0.99999
4f_sze_l	8534	0.04762
4f_ww_l	184.7	0.99999
2f_z_l	929.6	0.65653
2f_z_h	5270.8	0.02317
2f_z_bhabhag	1580.1	0.02112
4f_ww_h	1812.0	0.02320
4f_ww_sl	2223.5	0.23174
4f_zzorww_h	1510.7	0.02320
4f_zz_h	167.4	0.02320
4f_zz_l	13.3	0.98921
4f_zz_sl	142.38	0.02311
4f_sw_l	1838.5	0.02242
4f_sw_sl	5503.9	0.22426
4f_sze_sl	2464.3	0.02061
4f_sznu_sl	1237.5	0.02320
4f_szorsw_l	950.4	0.02233
6f_ttbar	449	0.75790
Fast Simulation		
ea_ell	105041.2	0.10000
ae_ell	104896.4	0.99999
aa_4f	132.9	1.00000
5f	51.78	1.00001

Table 1: Summary of event generation samples. The quoted cross sections and integrated luminosity are referred to the beam polarisation state: (P_{e^-},P_{e^+})=(−0.8,+0.2), at sqrt(s)=1 TeV. The list of SM process with 4 fermions in the final state is exhaustive.

3.1 Signal Sample

The signal events used in this analysis have been created by generating events with a final state of $\nu_e\bar{\nu}_e H$ using `WHIZARD`. The decay of the higgs boson in `PYTHIA` was forced into two muons. The width of a 125 GeV/c^2 Standard Model Higgs is negligible compared with the invariant mass resolution of the detector. The topology of the event comprises two muons and missing energy. Figure 2 shows the Feynman diagrams to $e^+e^- \rightarrow \nu_e\bar{\nu}_e$H , H $\rightarrow \mu^+\mu^-$ in the ILC. In this analysis the contribution from Higgsstrahlung is negligible compared with WW-fusion.

3.2 Main Backgrounds

The main background comes for those processes with final state $\nu\bar{\nu}\mu^+\mu^-$, where the pair of muons are not from a Higgs decay. The initial state could be e^+e^- or $\gamma\gamma$. The ratio of the production cross

Figure 2: Feynman diagrams for signal: Higgsstrahlung (left) and WW-fusion (right). The WW-fusion is the dominant process at 1 TeV and (P_{e^-}, P_{e^+})=(-0.8,+0.2). In this analysis, the contribution from Higgsstrahlung process is negligible compared with WW-fusion.

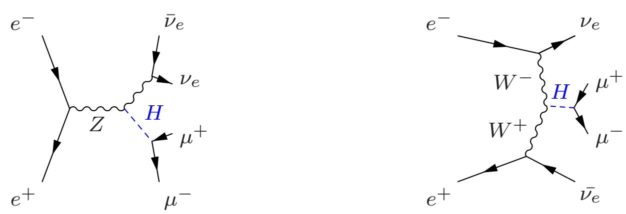

sections between these backgrounds and signal exceed 10^3. Table 1 list all the cross sections for those backgrounds.

4 Event Selection

The event selection is done in two steps. First, preselection of the events with two large energy muons in the final state, with invariant mass around to the Higgs mass peak. The final selection cuts are obtained by means an optimization process.

4.1 Preselection

Only events with two reconstructed muons with $E > 15$ GeV are used. The identification of the muons is based on the deposited energy over the calorimeters. Objects not being produced in the primary vertex. are rejected with the requirement $|d_0/\Delta d_0| < 5$.

The missing energy of the event $\not{E}$ is defined as the center-of-mass energy less the total observed energy. A minimum value of $\not{E}$>300 GeV is required to accept the event. The hadronic/semileptonic modes are rejected requiring less than 4 charged PFO's with energy higher than 15 GeV , and less than 3 leptons with $E > 15$ GeV. Table 2 shows the preselection cuts. No isolation requirement is made. The signal efficiency after these preselection requirements is 85 %.

Muons
charged PFO
$E > 15$ GeV
$E_{calE}/(E_{calE} + E_{calH}) < 0.5$
$(E_{calE} + E_{calH})/\|\vec{P}\| < 0.3$
$\|d_0/\Delta d_0\| < 5$
Dimuon system
Opposite sign charges
$E_{muon1} + E_{muon2} < 400$ GeV
$\|M(\mu^+, \mu^-) - 125\| < 30$ GeV/c^2
$\not{E} > 300$ GeV
charged PFO's with $E > 15$ GeV< 4
charged leptons with $E > 15$ GeV< 3

Table 2: Preselection cuts: E_{calE} (E_{calH}) is the deposited energy on the electromagnetic (hadronic) calorimeter by the muon, P is the momentum of the muon and d_0 its impact parameter. The cut on the maximum energy of the dimuon system select one of the process (WW-fusion) in Fig. 2.

4.2 Optimization

A cut based selection is performed using the following variables: $\not{E}_T, \not{E}$, $\mathrm{P_T}(\mu^+)+\mathrm{P_T}(\mu^-)$, $\mathrm{P_T}(\mu^+,\mu^-)$, $cos(\mu^+,\mu^-)$. Optimization of the final cuts is performed using as score function the significance defined by:

$$\frac{S}{\sqrt{S+B}} \tag{1}$$

where S is the number of signal events passing selection on every scan with dimuon invariant mass inside $(124, 126)$ GeV/c^2; B is the number of background events inside sidebands (normalized to the signal window size). The sidebands are defined as: $(115, 120)$ and $(130, 135)$.

- Variables are scanned until we rise a **stable point**.
  - $\mathrm{var}_1 \rightarrow\ \mathrm{var}_2 \rightarrow\ \mathrm{var}_{N-1} \rightarrow\ \mathrm{var}_1$
  - If the var_i best value changes we scan var_1 again.
  - If no variables change in a full cycle ($\mathrm{var}_1 \rightarrow\ \mathrm{var}_1$): we found a stable point.
- A new variable is added var_N and we scan it.
- New cycle of scans to find a new stable point: $\mathrm{var}_1 \rightarrow\ \mathrm{var}_2 \rightarrow\ \mathrm{var}_N \rightarrow\ \mathrm{var}_1$

The performed scans are included in Appendix C. After the last scan the significance (Eq. 1) reaches ≈ 2.3.

Table 3 summarizes the optimization results. A requirement on the maximum energy deposited on the forward calorimeters is added to supress background contributions as $\gamma e^{\pm} \rightarrow ell\nu\nu$, $\gamma\gamma \rightarrow ll\nu\nu$. Figure 3 shows the dimuon invariant mass distribution before and after optimization.

Table 3: Result of the optimization.

$\not{E}_T > 40$ GeV
$\not{E} > 550$ GeV
$\mathrm{P_T}(\mu^+)+\mathrm{P_T}(\mu^-) > 130$ GeV/c
$cos(\mu^+,\mu^-) > -0.45$
BCal < 70 GeV

5 Branching Ratio Precision

In Section 4.2 it is shown that a statistical significance around $\sigma \approx 2.3$ is reached after the optimization process. This correspond with a statistical precision $\frac{\Delta(\sigma\cdot Br)}{\sigma\cdot Br} = \frac{1}{\sigma} \approx 43$ %; similar value can be obtained from the data after applying the final selection: defining a signal mass window (124, 126) GeV/c^2 the signal (background) contribution inside this window is $S = 14.95$ ($B = 21.96$), thereby we estimate the precision to be $\sqrt{S+B}/S \approx 41$ %.

This value is sensitive to fluctuations in the number of events; signal sample was obtained from high statistics Monte Carlo samples, but the simulated statistics for the background is lower.

Figure 3: Dimuon Invariant Mass after preselection (left) and after optimization (right).

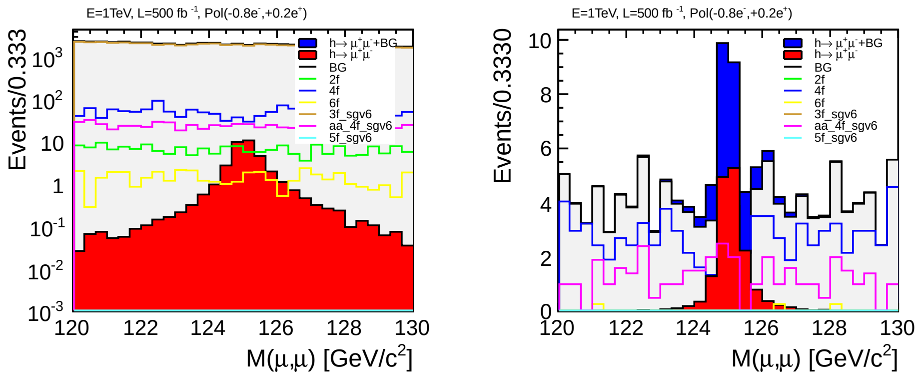

5.1 Pseudoexperiments

The background after optimization is flat (Fig. 3 with a value ≈ 4. A number of 10^5 independent background toy-samples were randomly generated using the background from data as template. For every sample, the value B of events inside (124, 126) GeV/c^2 is extracted and use to fill the distribution $\sqrt{S+B}/S$ [1].

Figure 4 shows the distribution $\sqrt{S+B}/S$ over all these pseudoexperiments with S (B) the number of signal (background) events within the mass window (124, 126) GeV/c^2 . A gaussian fit return the values: mean = 0.44, $\sigma = 0.015$.

Figure 4: Distribution $\sqrt{S+B}/S$ over all the pseudoexperiments; S (B) are the signal (background) events passing selection with invariant dimuon mass inside (124, 126) GeV/c^2.

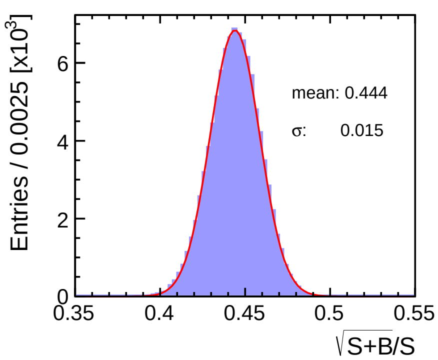

6 Results

In Section 4.2 the statistical significance for $\sigma \cdot Br$ is estimated as $41 - 43$ %. This value is obtained directly from the data samples after the final selection, and it is sensitive to fluctuations in the observed number of events.

[1]The number of signal events, S, is the one observed on the data sample

In Sec. 5 an alternative toy Monte Carlo based approach is followed: many independent background samples are randomly generated from the background shape observed in the data. The number of signal events on the data, S, and the number of background events on every of the toy samples, B, both inside a mass window (124, 126)GeV/c^2 are used to fill the distriution $\sqrt{S+B}/S$ (4). The expected statistical precision for $\sigma \cdot Br$ is estimated as $\pm 2\sigma$ of the peak value of that distribution, thereby, $\frac{\Delta(\sigma \cdot Br)}{\sigma \cdot Br} = 44 \pm 3$ %.

7 Conclusion

The statistical uncertainty for a measurement of the cross section times branching ratio of a light Standard Model Higgs boson, with a mass of 125 GeV/c^2 decaying into two muons has been evaluated. At the ILD, with a center-of-mass energy of 1 TeV , beam polarisation state (P_{e^-}, P_{e^+})=(-0.8,+0.2), and total integrated luminosity of 500 fb^{-1}, $\frac{\Delta(\sigma \cdot Br)}{\sigma \cdot Br} \sim 44 \pm 3$ %.

A Samples Description

This appendix list the final state of the samples used in this analysis.

In the final states of the 6f_ttbar samples:

- e refers to an electron-positron and l other charged lepton.
- v refers to one neutrino.
- x is up-type quark and y is down-type quark (Some channels have one or more final quarks given explicitly).
- ae_ell, ea_ell, aa_4f and 5f samples were generated with fast simulation.
- All other samples were fully simulated.

Full detail about all these samples can be found in [12].

Label	Process
hmumu	$e^-e^+ \rightarrow \nu_e\bar{\nu}_e\mathrm{H}, \mathrm{H} \rightarrow \mu^+\mu^-$, (signal)
4f_sznu_l	$e^-e^+ \rightarrow \nu_e\bar{\nu}_e\, l^+l^-; \quad l = \mu, \tau$
4f_zzorww_l	$e^-e^+ \rightarrow \nu_l\bar{\nu}_l\, l^+l^-; \quad l = \mu, \tau$
4f_sze_l	$e^-e^+ \rightarrow e^+e^-l^+l^-$, $e^-e^+ \rightarrow \nu_i\bar{\nu}_i e^+e^-; \quad i = \mu, \tau; \, l = e, \mu, \tau$
4f_sw_l	$e^-e^+ \rightarrow \nu_\tau\tau^+\bar{\nu}_e e^-$
4f_zz_l	$e^-e^+ \rightarrow l^-l^-l^+l^+, \nu_i\bar{\nu}_i l^-l^+; \, i, l = \mu, \tau$
4f_ww_l	$e^-e^+ \rightarrow \nu_\mu\mu^+\bar{\nu}_\tau\tau^-$
4f_szorsw_l	$e^-e^+ \rightarrow \nu_e e^-e^+\bar{\nu}_e$
2f_z_l	$e^-e^+ \rightarrow l^+l^-; \quad l = \mu, \tau$
2f_z_h	$e^-e^+ \rightarrow q\bar{q}; \quad q = u, d, s, c, b$
2f_z_bhabhag	$e^-e^+ \rightarrow e^+e^-\gamma$
ww_h	$e^-e^+ \rightarrow q_1q_2\bar{q}_2\bar{q}_1; \, q_1 = u, c; \, q_2 = d, s$
4f_zz_h	$e^-e^+ \rightarrow q_1\bar{q}_1q_2\bar{q}_2, q_1\bar{q}_1q_2\bar{q}_3; \, q_1 = u, c; q_2, q_3 = d, b$ $e^-e^+ \rightarrow q_1q_1\bar{q}_1\bar{q}_1, q_1q_2\bar{q}_1\bar{q}_2 \, q_1 = d, s, b; q_2 = d, s, b$ $e^-e^+ \rightarrow q_1q_1\bar{q}_1\bar{q}_1, q_1q_2\bar{q}_1\bar{q}_2 \, q_1 = u, c; q_2 = u, c$ $e^-e^+ \rightarrow q_1\bar{q}_1q_2\bar{q}_2, q_1\bar{q}_1q_2\bar{q}_3; \, q_1 = u; q_2, q_3 = s, b$
4f_ww_sl	$e^-e^+ \rightarrow q_1\bar{q}_2l^-\bar{\nu}_l; \, q_1 = u, cq_2 = d, b, s; l = \mu, \tau$
4f_zz_sl	$e^-e^+ \rightarrow \mu^-\mu^+q_1\bar{q}_1, q_2\bar{q}_2\mu^-\mu' \nu_l\bar{\nu}_l q_1\bar{q}_1, ; \, q_1 = u, c; q_2 = d, s, b; l = \mu, \tau$ $e^-e^+ \rightarrow \nu_l\bar{\nu}_l q_2\bar{q}_2, q_2\bar{q}_2\tau^-\tau^+; \, q_2 = d, s, b; l = \mu, \tau$
4f_sw_sl	$e^-e^+ \rightarrow q_1\bar{q}2e^-\nu_e; \, q_1 = u, c; \, q_2 = d, s, b$
4f_sznu_sl	$e^-e^+ \rightarrow \nu_e\bar{\nu}_e q_1\bar{q}_1, \nu_e\bar{\nu}_e q_1\bar{q}_2; \, q_1, q_2 = b, s, c, d, u(Q(q_1) = Q(q_2))$
4f_sze_sl	$e^-e^+ \rightarrow {}^-e^q_1\bar{q}_1, q_1\bar{q}_1e^-e^; \, q_1 = u, c$
6f_ttbar	yyveev yyvelv yyveyx yyvlev yyvllv yyvlyx yyxyev yyxylv yyuyyu yyuyyc yycyyu yycyyc
ea_ell	$e^-\gamma \rightarrow e^+\, l^+l^-$, $l = \mu, \tau$
ae_ell	$\gamma e^+ \rightarrow e^+\, l^+l^-$, $l = \mu, \tau$
aa_4f	$\gamma\gamma \rightarrow \nu_e\bar{\nu}_e\, l^+l^-; \quad l = \mu, \tau$
5f	$e^+l^+l^-\nu_i\bar{\nu}_i; \, l = \mu, \tau; i = e, \mu, \tau$ $e^+l_1^+l_2^-\nu_i\bar{\nu}_i; \, l_1, l_2 = \mu, \tau; i = e, \mu, \tau$

B Event Distributions

This appendix contains the event distributions after preselection.

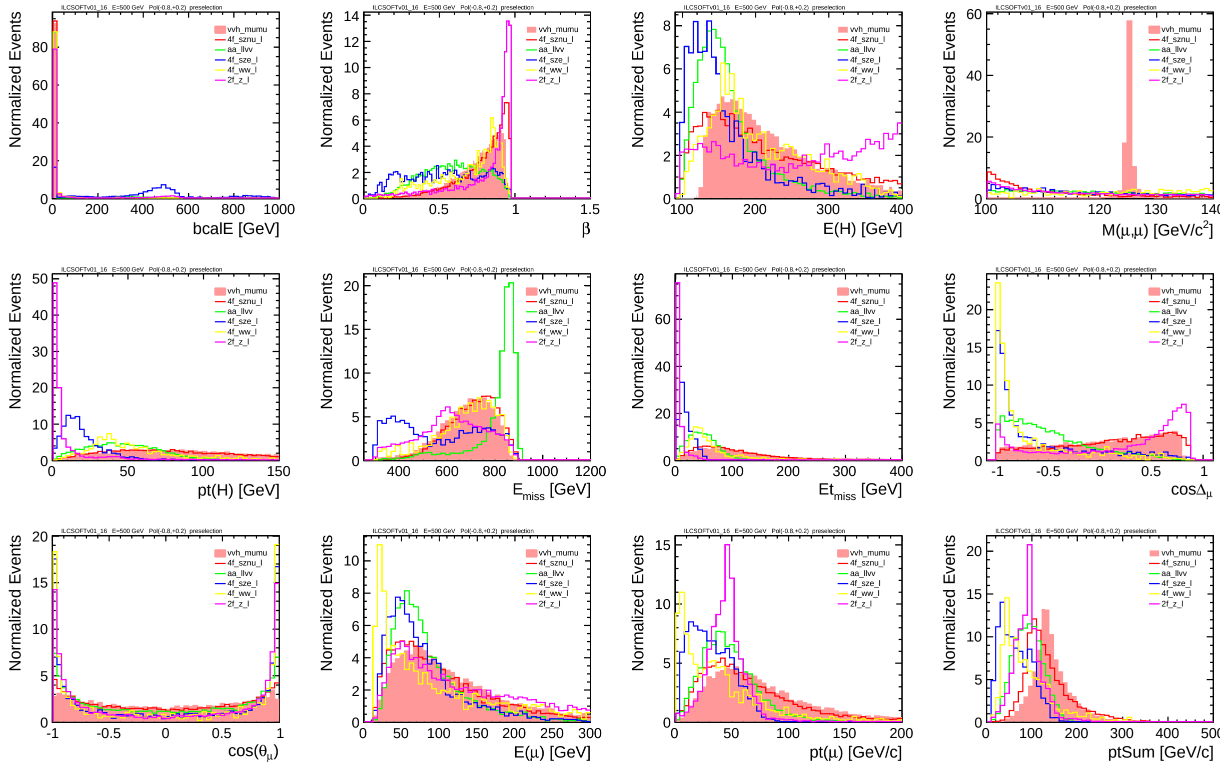

C Optimization Scans

This appendix contains the steps in the optimization process.

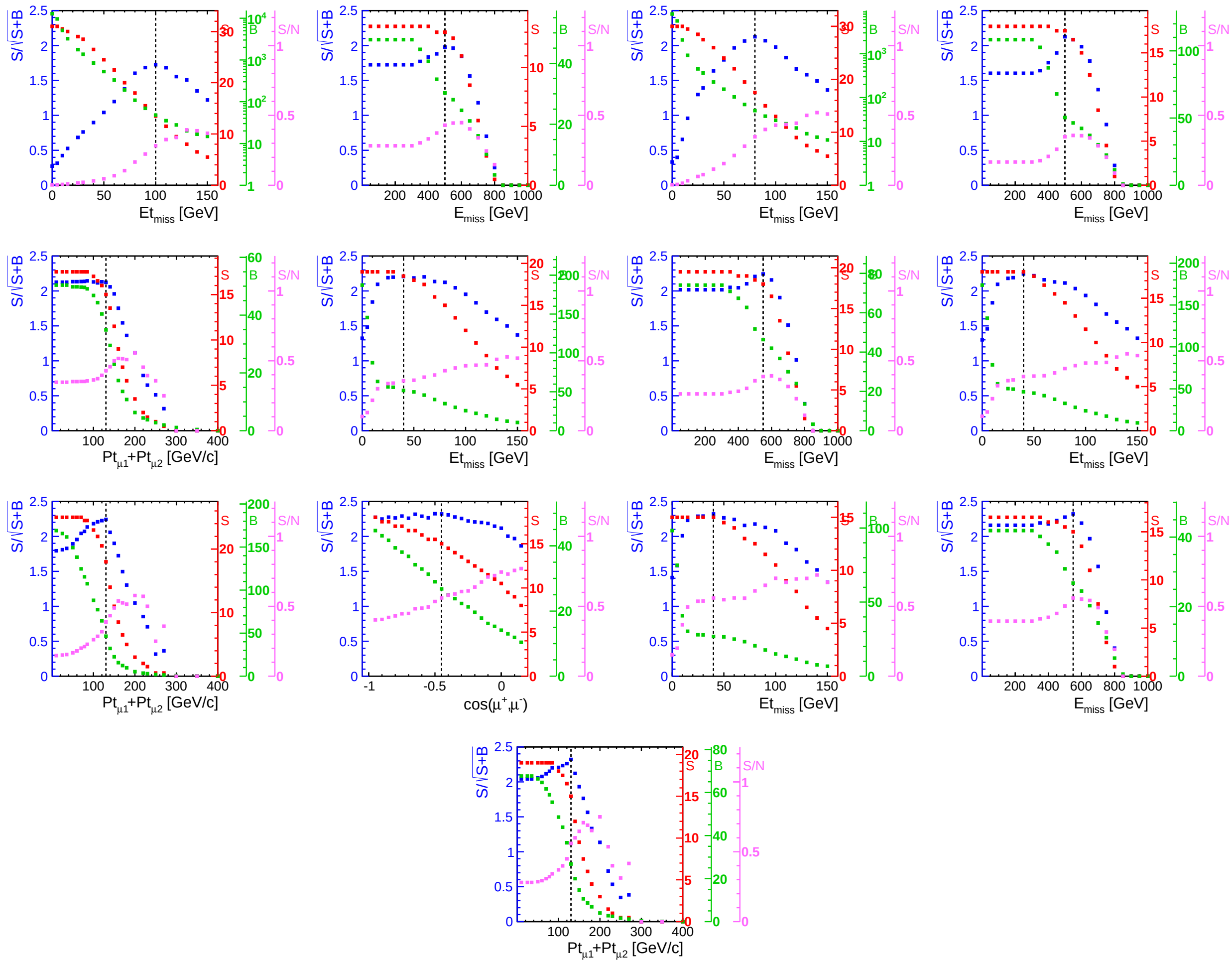

D Event Distributions After Optimization

This appendix contains the event distributions after optimization.

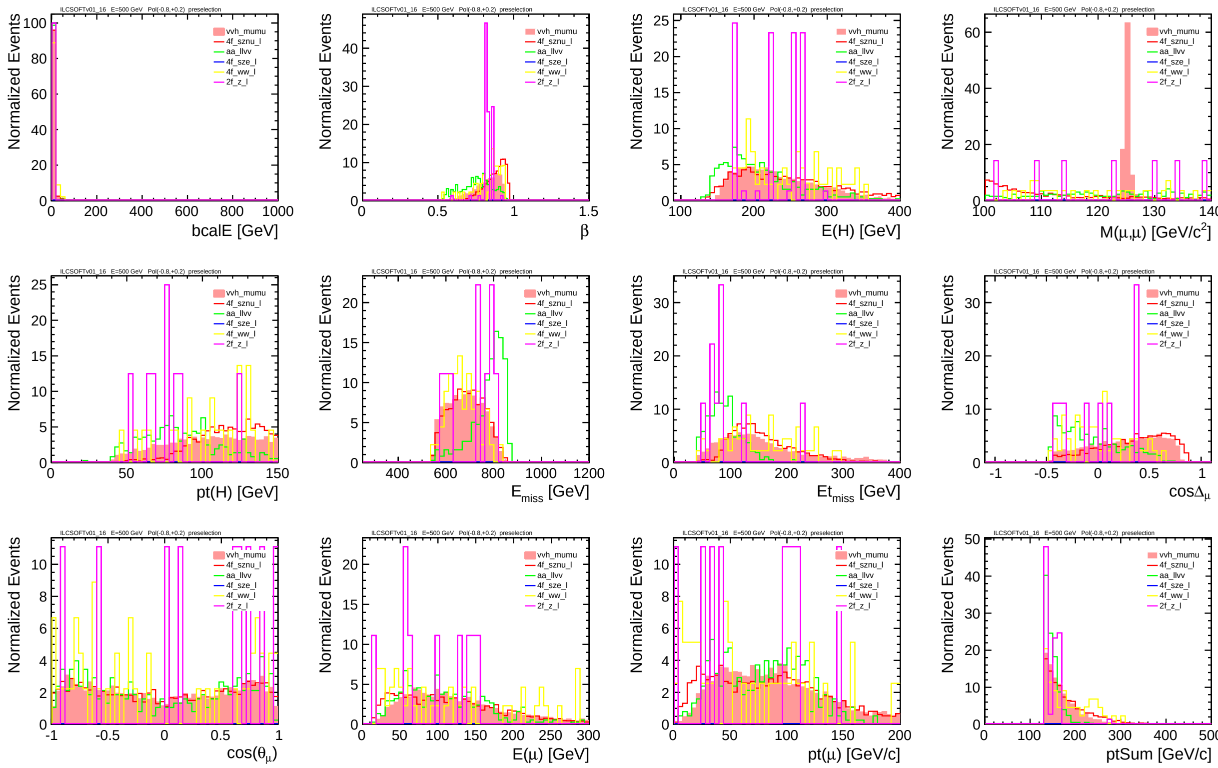

E Cut Flow Table

This appendix contains the analysis cut table. The quoted number of events referes to the **Monte Carlo statistics** (no applied weights); it includes all the beam polarisation states contribuing to the current process. The efficiency for every process can not be obtained just as the ratio of two columns. In order to obtain the efficiency it is necessary separate all the pure polarisation states taking in account their different cross sections. Thereby, the efficiency is defined as:

$$\frac{N_{obs}}{N_{exp}}$$

with N_{obs} (N_{exp}) the total number of observed (expected) events under the experimental conditions, that is, $L = 500$ fb^{-1}and beam state polarisation (P_{e^-}, P_{e^+})=(-0.8,+0.2). The efficiency is included in the last column.

Sample/Cut	generated	preselection	missEt	missE	ptSum	cosD	bcalE	effi
vvh_mumu	19800	10839	9553	8290	5948	5122	4943	.318356
4f_sznu_l	477413	11004	9163	8335	4171	3795	3734	.039122
4f_sze_l	1611426	2309	152	7	1	0	0	0
2f_z_h	338147	5	0	0	0	0	0	0
2f_z_l	2106528	9946	241	132	28	9	9	.000003
4f_sw_l	87453	11	10	7	1	1	1	.000002
4f_sw_sl	2611402	6	3	3	0	0	0	0
4f_ww_h	78039	5	0	0	0	0	0	0
4f_ww_l	343337	1048	680	540	134	46	45	.000632
4f_ww_sl	957247	970	410	40	3	1	1	.000001
4f_zz_h	9671	1	0	0	0	0	0	0
4f_zz_l	37386	352	169	112	42	37	33	.000007
4f_zzorww_h	65524	4	0	0	0	0	0	0
4f_zzorww_l	360269	2685	1776	1499	703	285	253	.001985
4f_zz_sl	8316	16	1	0	0	0	0	0
yycyyc	329537	2	1	0	0	0	0	0
yycyyu	137616	3	0	0	0	0	0	0
yyuyyc	138426	3	1	0	0	0	0	0
yyuyyu	139987	1	0	0	0	0	0	0
yyvelv	42873	30	22	7	1	0	0	0
yyveyx	140251	2	2	0	0	0	0	0
yyvlev	42869	4	4	1	0	0	0	0
yyvllv	53867	664	569	193	69	27	26	.001111
yyvlyx	193651	292	220	6	1	1	1	.000042
yyxyev	170823	3	2	0	0	0	0	0
yyxylv	193929	272	214	12	2	0	0	0
ae_ell	10489608.00	67767	3797	134	5	4	2	0
ea_ell	10504152.00	68295	3929	140	4	1	1	.000015
aa_4f	132939	7531	4513	4213	762	410	357	.000751
ae_ellvv	10356.60	450	289	197	37	25	11	0
ea_ellvv	15526.80	466	299	208	41	28	16	.001544

References

[1] ILC Project, A. Djouadi et al., eds., "International Linear Collider Reference Design Report Volume 2: Physics at the ILC." 2007. arXiv:0709.1893 [hep-ph]. ILC-REPORT-2007-001.

[2] "The International Large Detector: Letter of Intent." arXiv:1006.3396 [hep-ex].

[3] W. Kilian, T. Ohl, and J. Reuter. "WHIZARD: Simulating multi-particle processes at LHC and ILC." 2007. arXiv:0708.4233v1 .

[4] T. Sjostrand, S. Mrenna, and P. Z. Skands. "PYTHIA 6.4 Physics and Manual." *JHEP*, vol. 05 p. 026, 2006. hep-ph/0603175.

[5] Z. Was. "TAUOLA the library for tau lepton decay, and KKMC/KORALB/KORALZ/... status report." *Nucl. Phys. Proc. Suppl.*, vol. 98 pp. 96102, 2001. hep-ph/0011305.

[6] S. Agostinelli et al. "Geant4 A Simulation Toolkit." *Nucl. Instrum. Methods Phys.* Res., Sect. A, vol. 506(3) pp. 250303, 2003.

[7] http://ilcsoft.desy.de/portal/.

[8] R. Brun and F. Rademakers. "ROOT – an object oriented data analysis framework." *Nucl. Instrum. Methods Phys.* Res., Sect. A, vol. 389(1-2) pp. 8186, 1997.

[9] A. Hocker, et al. "TMVA – Toolkit for multivariate data analysis." 2009. arXiv:physics/0703039.

[10] Verkerke and D. P. Kirkby. "The RooFit toolkit for data modeling." 2003. arXiv:physics/0306116.

[11] M. Berggren, SGV 2.31 - A fast and simple program for simulating high energy physics experiments at colliding beam detectors. http://berggren.home.cern.ch/berggren/sgv.html

[12] http://ilcsoft.desy.de/dbd/generated/